Structural analysis of an automotive forming tool for large presses using LS-DYNA

K. Swidergal[1], C. Lubeseder[2], I. von Wurmb[2], A. Lipp[2], J. Meinhardt[2], M. Wagner[1], S. Marburg[3]

[1]Ostbayerische Technische Hochschule Regensburg, Mechanical Engineering Department, Laboratory for Finite Element Analysis and Structural Dynamics, Galgenbergstraße. 30, 93053 Regensburg, Germany
[2]BMW Group, Construction methods and Standards Department, Knorrstraße 147, 80788 Munich, Germany
[3]Universität der Bundeswehr München, LRT4 – Institute of Mechanics, Werner-Heisenberg-Weg 39, 85577 Neubiberg, Germany

1 Abstract

To improve efficiency in automotive press shops, press systems with increasingly high stroke rates are being implemented, raising thereby the structural dynamic load on the press and especially on the forming tool. In this paper, the detailed knowledge about the tool's deformation, which is essential for an accurate and robust design of forming tools, is gained by conducting a structural dynamic finite element method (FEM) simulation of a selected automotive tool. Starting with a simplified press model, which accounts for the elasticity of the press support and the slide cushion, the FE model is extended with the forming tool assembly. The focus in the presented model is put on one of the tool's components, namely the forming slide. The transient simulation of one forming cycle is preceded by a dynamic relaxation phase where the gravity load is applied and the gas springs are pre-stressed. The model is built with ANSA preprocessor and solved with LS-DYNA explicit. For validation of the simulation results, the kinematic responses of the slide are compared with the measurements obtained in an experiment.

2 Introduction

Due to high investment costs of an automotive forming tool for large presses, the tool designers are trying to integrate as much forming operations in one tool as possible, reducing therefore their overall number [1]. As a side effect, the modern tools are getting more and more complex. Moreover, due to the press systems with increasingly high stroke rates [2] and a growing usage of high strength steels [3] the structural dynamic loading on those tools increases. Therefore, to gain a detailed knowledge of deformations and thus enable an accurate and robust design of complex forming tools numerical simulation can be advantageously applied [4]. This has already been shown in [5], where a coupled multibody finite element simulation (MBS-FEM) approach for analyzing the vibration of the blankholder was presented. In this work, a structural FEM analysis of a selected automotive tool using LS-DYNA is conducted. To correctly consider the tool's mounting boundary conditions, as investigated in [6], an additional simplified press model is used, which accounts for the press support's elasticity and the slide cushion's elasticity. The focus in the presented model is put on one of the tool's components, namely the forming slide. Therefore, in the following section a short description of its function is given.

2.1 Working principle of the forming slide

Not all forming or trimming operations can be carried out with the vertical movement of the punch only. There is a limitation of the maximal allowed tilt angle of the workpiece [1] during the processing. Hence, if the forming of complex-shaped blank sheet requires a greater angle, then the part needs to be reoriented – with the drawback of extra transportation cost and time, or – alternatively – forming or trimming slides can be employed. The forming slide transforms the vertical movement of the press slide into horizontal or inclined movement of the slide, using the principle of an inclined plane. In Figure 1, the schematic view of the automotive forming follower press tool equipped with the forming slide is shown. Additionally, the main events during one operating cycle are presented. The tool consists basically of two halves, the upper and lower die, which are fixed to the press slide and press bed accordingly. The lower die holds the matrix with the preformed blank sheet on it and the forming slide which can move

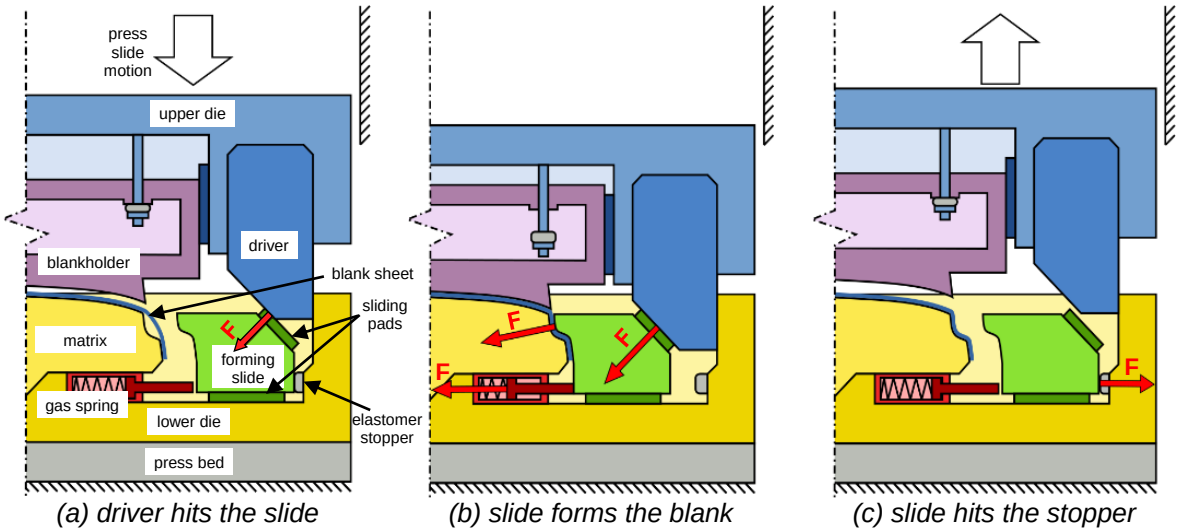

Fig.1: Main events during operating cycle of the forming slide.

translationally on the sliding pads. The upper die hosts the wedge-formed driver which pushes the forming slide and the blankholder. The press cycle begins with the press slide moving downwards, as depicted in Figure 1a. Prior to the actual forming, the blank sheet is secured with the blankholder. At the same time, the forming slide is pushed by the driver towards the workpiece and against the pre-stressed gas spring. Then the press slide continues moving downwards and draws the blank into the die, see Figure 1b, so that the component obtains its desired shape. After the forming process is completed, the press slide moves back up to its original position removing the blankholder and allowing the forming slide to return. To avoid hard impacts, elastomer stoppers are used, which are made of highly nonlinear filled elastomer and should absorb the kinetic energy of the returning forming slide, as shown in Figure 1c. At the end, the finished piece is removed and the cycle repeats.

3 Developing the LS-DYNA model

The FE model of the investigated forming tool is set-up within the ANSA environment, a general finite element preprocessor [7]. Due to the large number of geometrical parts, the model is organized into several subassemblies. In Figure 2, for example, the forming slide assembly, with its main components described, can be seen.

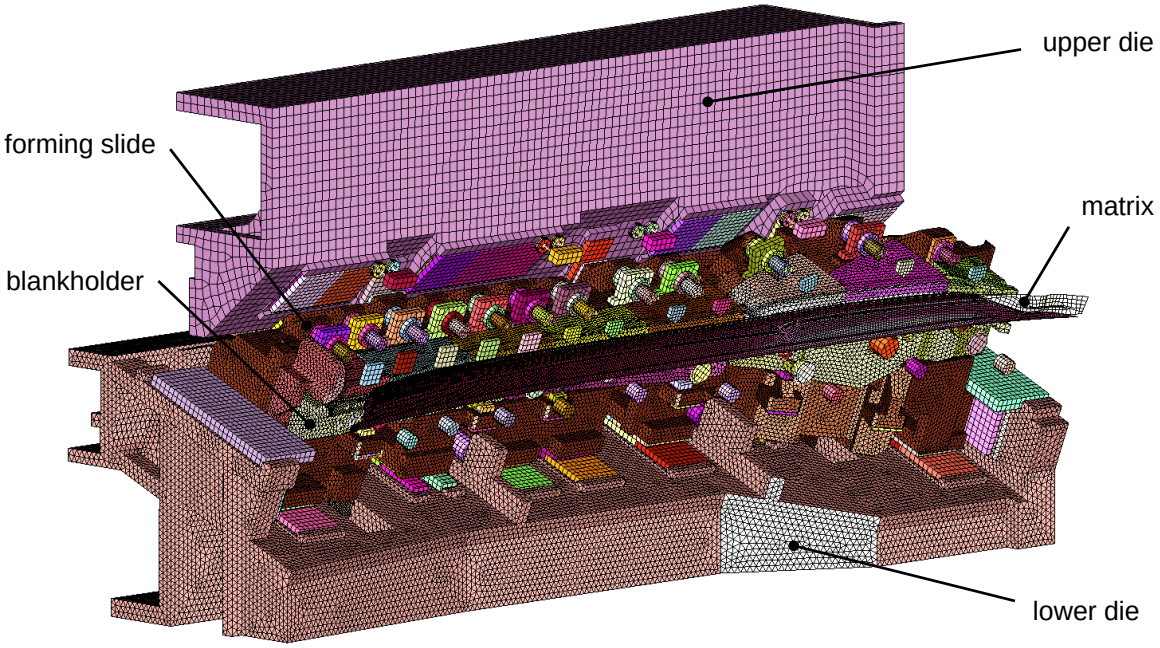

Fig.2: LS-DYNA model of the forming slide assembly.

3.1 Model discretization

All CAD geometries are defeatured, allowing for easier and more uniform meshing. The vast majority of parts is discretized with constant stress under-integrated hexahedral elements (**ELFORM=1**) using the mapped meshing algorithm. Other parts, like complex-shaped iron cast structures are meshed with linear tetrahedral elements with nodal pressure averaging formulation **ELFORM=13**, which significantly lowers the volumetric locking [8]. Prior to batch meshing, adequate quality criteria like the element minimal size, the aspect ratio and the skewness are set, resulting in an overall good quality mesh for explicit simulation. Attention is paid, that the critical features like fillets of sliding pads or guide pillars are sufficiently discretized. For representing the strings and dampers, discrete elements are used. Some irrelevant parts like e.g. bodies of the pneumatic actuators are removed, and their mass is added to their hosting components using the ***ELEMENT_MASS** keyword.

3.2 Materials

All parts, for which elasticity could play a relevant role in the distribution of forces in the tool, like cast iron structures, punches, sliding pads or press bed are considered to be elastic. They are modeled with the ***MAT_PIECEWISE_LINEAR_PLASTICITY** material model, with their material properties provided. In Table 1, for example, the necessary properties defining the forming slide's material EN-GJS-600-3 are listed.

Property	Unit	Value
Mass density, **RO**	to/mm³	7.2e-9
Young's modulus, **E**	MPa	174000
Poisson's ratio, **PR**	-	0.275
Yield strength, **SIGY**	MPa	370
Tangent modulus, **ETAN**	MPa	76

Table 1: Material properties of the forming slide body (EN-GJS-600-3).

By means of the parameter **SIGY** and **ETAN** a simplified yield curve is specified. Even if the expected deformation are lying within the elastic limit, it is still advisable to work with the plastic material model, as it is useful for debugging purposes during the model development. It can also be beneficial, if an accurate prediction of the tool deformation at critical situations like, for example, damage of the tool's component (breaking of the bolt) or intrusion of an external body into the tool should be simulated.
For rubber components like elastomer dampers, profiled cushioning bars, or polyurethane springs, a ***MAT_SIMPLIFIED_RUBBER** material model [9] is taken, which is a tabulated version of the Ogden hyperelastic material model. The necessary uniaxial stress-strain curves for several discrete strain rates, as shown in Figure 3, have been obtained experimentally, see [10], and provided in a table definition.

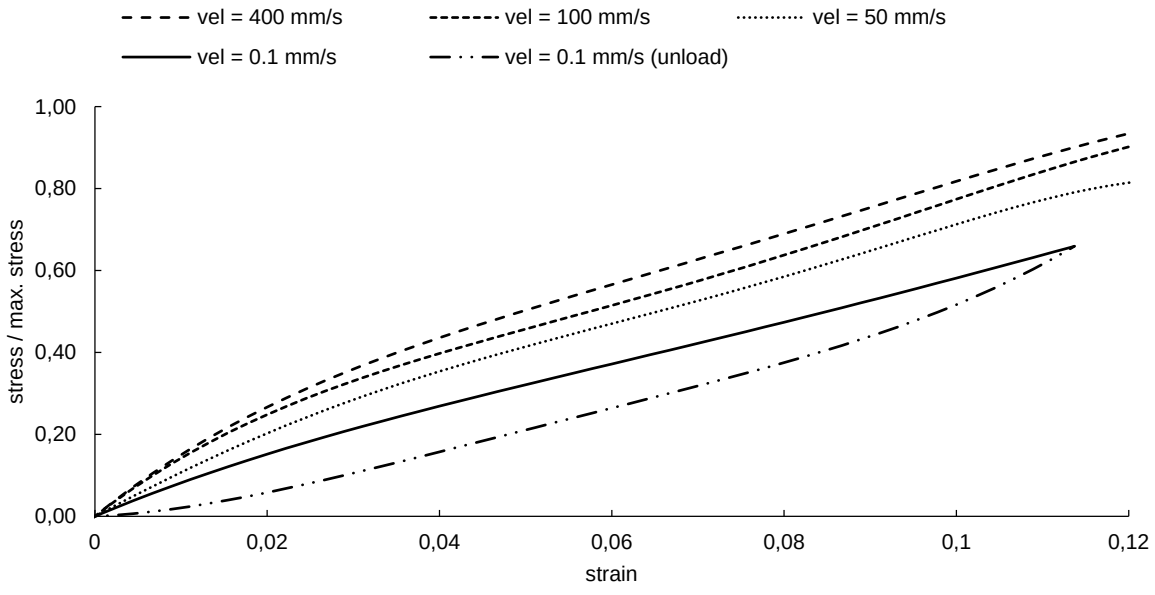

*Fig.3: Uniaxial stress-strain curves of the elastomer stoppers used in ***MAT_SIMPLIFIED_RUBBER**.*

All other parts are modeled rigidly. In cases, that only the dummy representation of the component is used (e.g. the press body) then the ***PART_INERTIA** card is taken for a proper mass definition.

3.3 Contact and connections

To correctly consider the tool's mounting conditions, an additional simplified press model, as shown in Figure 4, is used. It accounts for the press support's elasticity and the press slide cushion's elasticity and their damping behavior. Moreover, both, the press bed and the slide's mounting plate are deformable. The rigid press body is constrained vertically on the corresponding ***MAT_RIGID** card.

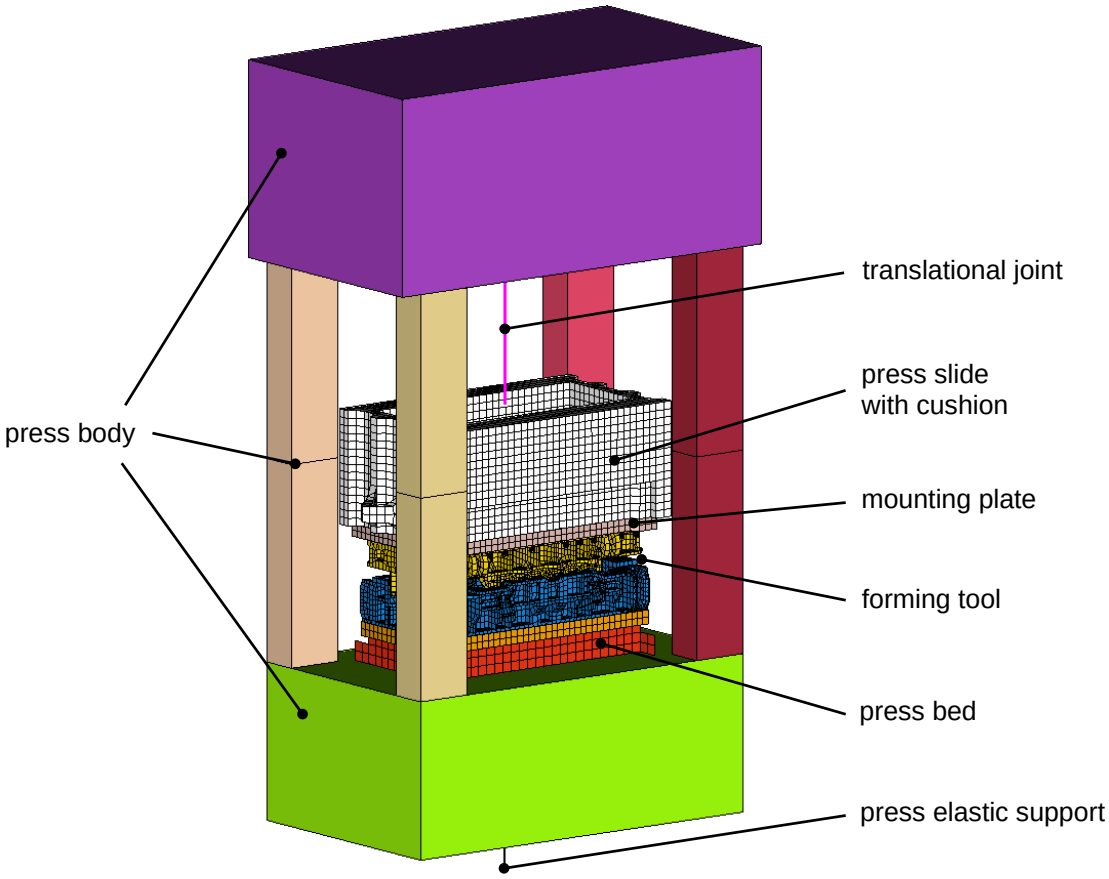

Fig.4: Simplified LS-DYNA model of the press.

Several constraining techniques are utilized to connect assembly components. If two rigid bodies have to be merged, then the ***CONSTRAINED_RIGID_BODIES** is used, with the pairs of slave-master bodies defined. This method is especially useful during the first phase of model development, as it allows – as long as the parts have the ***MAT_RIGID** assigned - for the temporary merging of subassembly components into one master part definition, which can then be easily constrained and simulated. For fixing the flexible bodies with rigid ones the ***CONSTRAINED_EXTRA_NODES** keyword is used, which is a very efficient method, as it reduces the number of model degrees of freedom. In all other situations the ***CONTACT_TIED_NODES_TO_SURFACE_OFFSET** card - which is based on the penalty contact formulation – is taken, to fix the part together.
If separation or tilting of the components, like for example between sliding pads, is to be considered, then the ***CONTACT_SURFACE_TO_SURFACE** and ***CONTACT_NODES_TO_SURFACE** contact definitions, are employed. In sliding contacts friction is activated. In addition, the viscous contact damping **VDC** is set to 20% to reduce the high-frequency oscillation in contact forces [8].
The relative motion between rigid parts is allowed by means of joints. The pillars, for example, are guided with the ***CONSTRAINED_JOINT_CYLINDRICAL** joint definition, and in the gas springs to allow the spring's piston to slide only along the cylinder axis, ***CONSTRAINED_JOINT_TRANSLATIONAL**, as shown in Figure 5, is used. The constraining method with the **CMO** parameter on the ***MAT_RIGID** card generally did not prove to be effective for parts that are changing their orientation during solution, as the constraint directions for the rigid body defined there are fixed, that is, not updated with time.

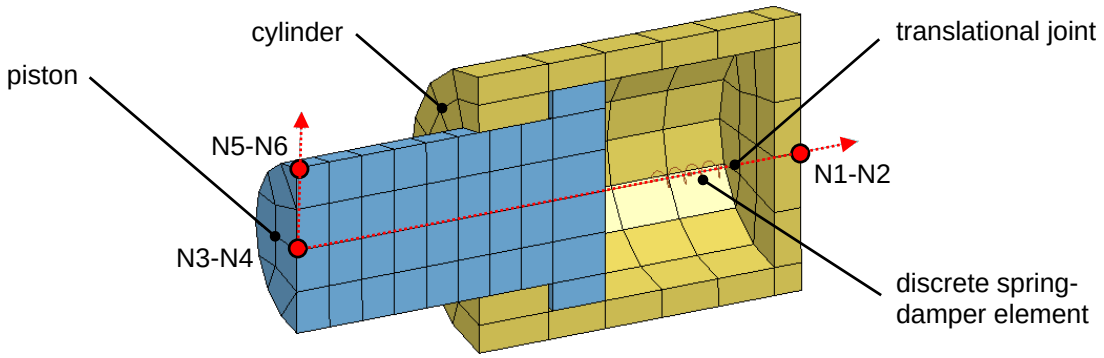

Fig.5: Cylinder and piston of a gas spring, constrained using translational joint.

For prescribing the motion of the press slide, initially the ***BOUNDARY_PRESCRIBED_MOTION_RIGID** card has been tried, with the option **VAD=4** which allows for providing the master rigid body (the press) to which the relative motion of the slave body (press slide) is acting. Unfortunately, with this option only a relative displacement curve can be provided, however this should be avoided in the explicit simulation. Therefore, a different approach is used, with the ***CONSTRAINED_JOINT_TRANSLATIONAL_MOTOR** joint card, where any of the displacement, velocity or acceleration curves can be used to define the motion. The input deck of this card is shown in Figure 6.

```
*CONSTRAINED_JOINT_TRANSLATIONAL_MOTOR_ID
$#     jid                                                          title
   1476994 press slide motion
$#      n1         n2         n3         n4         n5         n6        rps       damp
   1100000    1100002    1100001    1100003    1100004    1100005      0.000      0.000
$#    parm       lcid       type         r1
     0.000         99          1      0.000
```

*Fig.6: Structure of the card ***CONSTRAINED_JOINT_TRANSLATIONAL_MOTOR**.*

With the nodal pairs **N1-N2, N3-N4** and **N5-N6** the initial configuration of the translational joint is defined. The nodes are placed possibly far away from each other, to avoid numerical instabilities, as recommended in [8]. With **TYPE=1** the press slide's acceleration curve **LCID** is provided.

3.4 Loads and initial conditions

Applying the gravity load or pre-stressing the gas springs and bolts is done in the dynamic relaxation phase, which initializes stresses and deformation in a model to simulate a preload. In the chosen relaxation method an explicit analysis, damped by means of scaling nodal velocities by the factor 0.955 each time step [8], is performed. After the preloaded state is achieved, the time resets to zero and the normal phase of the solution automatically begins from the preloaded state. Due to very stiff spring constant of the press support, the chosen time step in the dynamic relaxation was very small, so that the convergence could not be obtained in reasonable time. To reach faster convergence the time step scaling factor **TSSDRF** on the ***CONTROL_DYNAMIC_RELAXATION** card is increased by 10. Pre-stressing of the elastomer stoppers is done with ***INITIAL_FOAM_REFERENCE_GEOMETRY** card, with the geometry of the elastomer defined in a deformed configuration.
The pneumatic cylinders are modelled with the ***DISCRETE_ELEMENT_LCO** card, which enables the variation of the spring's initial offset with time. In this way, through providing a displacement-time function the cylinders are actuated. In the material definition, a spring stiffness equal unity is chosen, hence the resultant actuator force equals the displacement offset in the discrete element.

3.5 Analysis settings

To stabilize the energy free modes of under-integrated hexahedral elements, the Belytschko-Bindeman stiffness hourglass control (type 6) is chosen. The simulation end time corresponds to one full stroke of the forming slide. To speed-up the computation time, mass scaling is activated. A time step size of 1.3e-6 sec is set, which – with the used mesh size – results in a 3% mass increase. The complete model is solved with explicit, SMP, double precision LS-DYNA R7.1.2 solver.
In the presented FE model, the blank sheet is not considered. The resulting response of the forming slide lacks therefore the effect of the process forming force. Nevertheless, as the events with the most dynamical loading on the tool, are starting either long before (driver hits slide) or long after (slide hits

stoppers) the actual forming process, the influence of the forming force on those events can be neglected, and their characteristic correctly obtained. Still, in the future, a model with the blank sheet inserted needs to be investigated.

4 Numerical aspects of the explicit simulation

During the model development, several numerical difficulties occurred, which result from the chosen explicit solving algorithm. Two aspects, the solver accuracy and proper selection of motion input curves will be briefly discussed here.

4.1 Solver accuracy

In the investigated model over 2 Mio cycles are necessary to complete the solution. As in explicit analysis numerical truncation may result in late time solution inaccuracy [8], the influence of the solver accuracy on the simulation results must be investigated. Therefore, the FE model is solved with both, a single- and a double-precision executable and the results are compared. In Figure 7, for example, a comparison of the press body vibration is shown. In both, the displacement and the velocity diagrams, at time about t = 0.5 sec, which corresponds to about 280,000 cycles, the curves obtained with a single-precision solver starts deviating from those run on a double-precision solver. Hence, in the investigated model the double precision LS-DYNA executable is used.

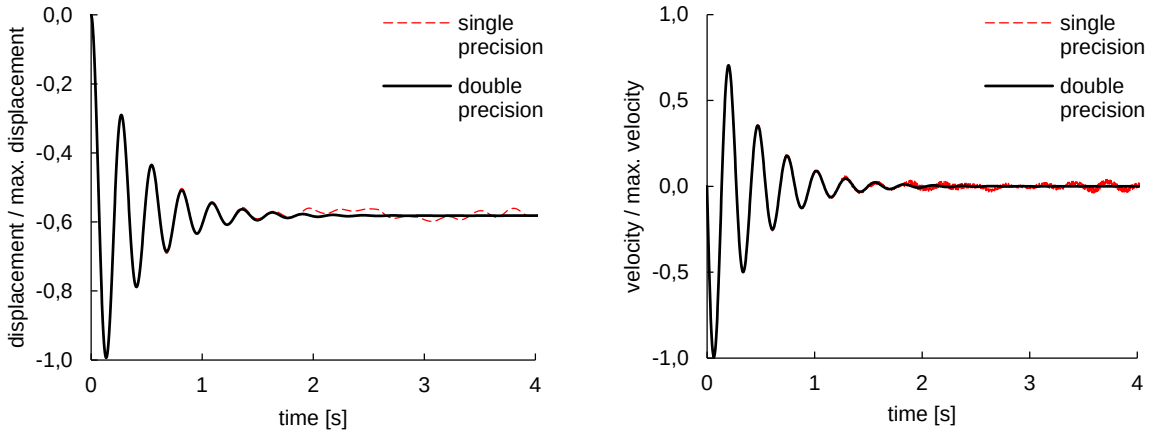

Fig.7: Comparison of the press body vibration solved using single and double precision solver.

4.2 Order of the motion input curve

To prescribe the motion of the press slide, a displacement, velocity or acceleration curve must be provided. In the explicit analysis the higher order kinematic quantities are preferable, therefore only velocity and acceleration curves are compared. The influence on the dynamics of the system can be well seen in the force plot. In Figure 8, for example, the reaction force in the translational joint of the press slide's cushion is shown. Due to differentiation, when the velocity input curve is used, peaks appear in the force function, causing artificial vibrations in the system. Hence, in the investigated model an acceleration curve is taken.

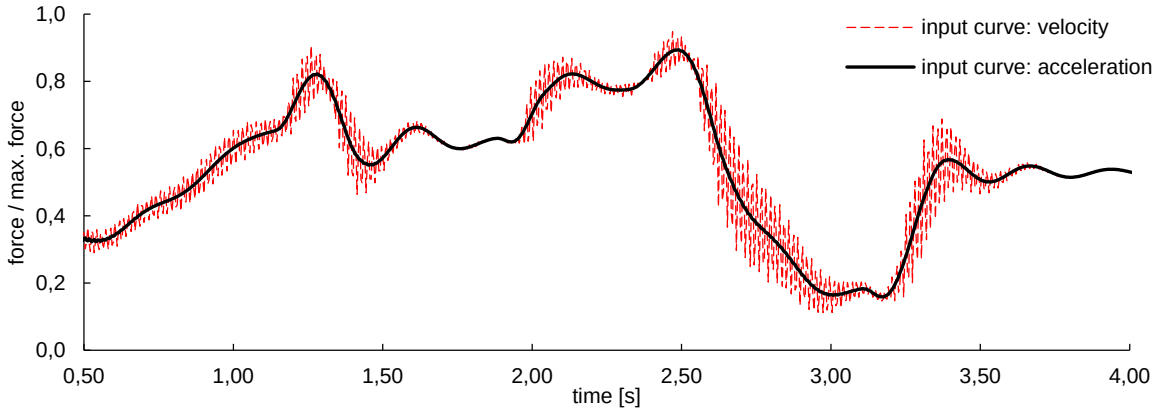

Fig.8: Comparison of the reaction force in the translational joint of the press slide's cushion for different input curves orders.

As the input curves defining motions are not rediscretized [8], the sampling of the input curve is varied and the influence on the results is investigated. For three sampling levels, 360, 1000 and 5000 points comparable results are obtained indicating that the chosen sampling is sufficient.

5 Results and discussion

In Figure 9, the normalized von Mises stress in the forming slide's body, as it is hit by the driver at time t = 1.41 s, is shown.

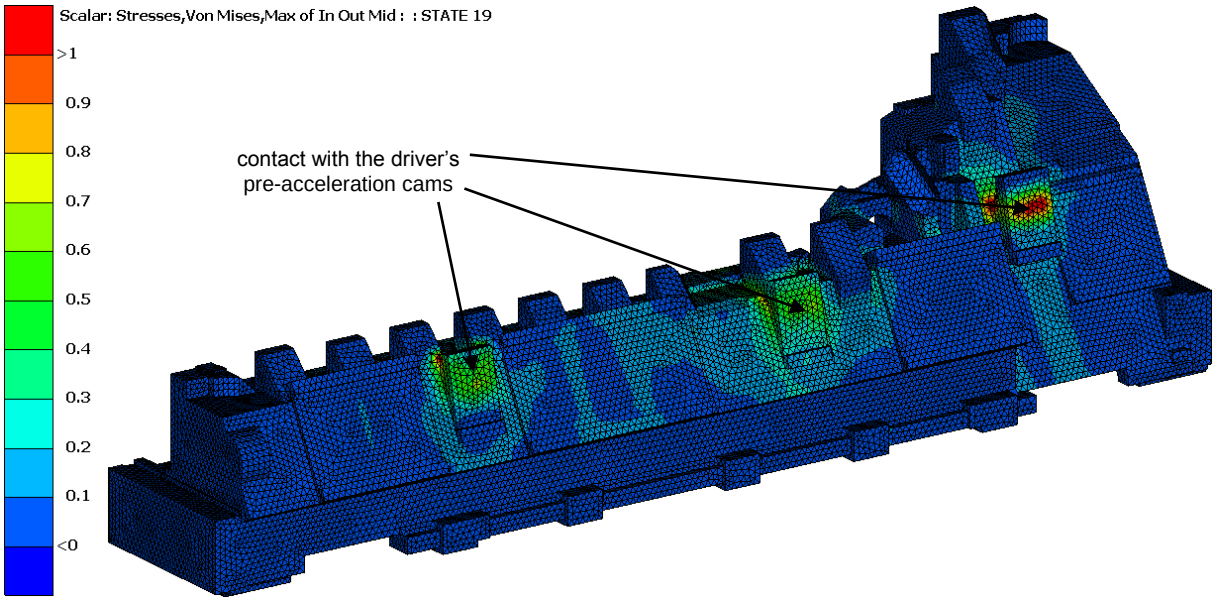

Fig.9: Normalized von Mises stress in the forming slide's body as it is hit by driver at time t = 1.41 s.

At places where the driver's pre-acceleration cams contact the slide's body, the regions of higher stress concentration can be identified. Moreover, the stress figure also indicates that in the model the contact pressure is not evenly distributed among the three sliding pads.
For the validation, the numerically obtained velocity response of the forming slide assembly was compared to the signal gained in an experiment, which was carried out under operational loading. Both velocity responses are shown in Figure 10.

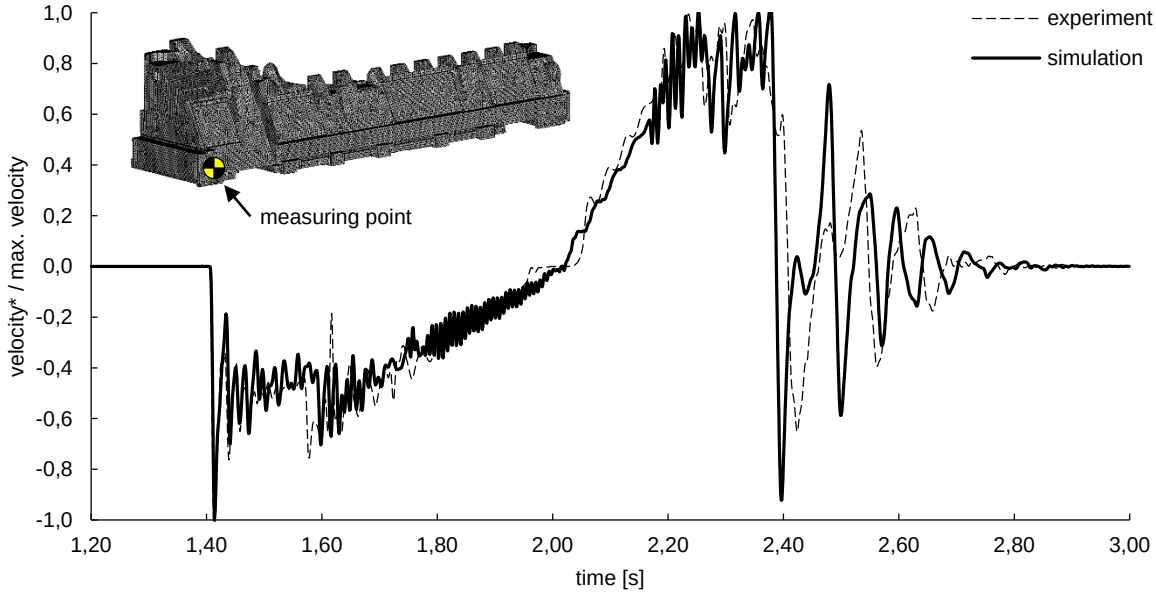

*Fig.10: Translational velocity of the forming slide (*lowpass, cutoff freq.: 100Hz) during its stroke.*

It can be seen, that the simulation results are in relatively good agreement with the measurements. During the travel of the forming slide, both velocity curves possess similar characteristic and their values lie within the same range. However, when the forming slide returns and hits the elastomer stoppers at time t~2.4s, it vibrates differently. The oscillations in the simulation begin about 10ms later, which can be explained with a different length of the elastomer stoppers used in the simulation and experiment. Due to the Mullins effect [11], the stoppers in the real tool have a reduced height, whereas in the FE model an initial unchanged length is used.

6 Conclusion and outlook

In this work, a structural FE analysis of the forming slide component in LS-DYNA was successfully conducted. Based on an experimental validation, the simulated resulting dynamic loading on the forming slide showed good agreement with measurements. In addition, the regions of critical stresses in the forming slide's body could be identified. Thanks to this knowledge, a deeper understanding about the forming slide behavior was gained. Hence, with this approach, more accurate and robust design of forming tools in the future is possible. Ultimately, the obtained component loads together with component stresses gained in a refined static FE analysis, can be used for fatigue life prediction. Besides, to make future tools lighter, a topology and shape optimization could then be conducted.

In the future, several refinements could be carried out, like e.g. considering the non-linear spring stiffness characteristic in the gas springs or activating more tool subassemblies at once. Also the influence of considering the blank sheet in the tool simulation to account for the forming process forces, as proposed in [12] could be investigated.
Furthermore, simulation time reduction should also be explored. Techniques like deformable to rigid switching, sub-cycling, selective mass scaling or implicit algorithm may bring considerable computational savings. Moreover, incorporating in the model the modal reduced parts **`*PART_MODES`**, which reference their frequency content stored in d3eigv and d3mode databases and are generated with the LS-DYNA implicit solver, should also be studied. Besides, the time needed for building the FE model can also be reduced by automating the developing process.

7 Literature

[1] Hoffmann, H.; Neugebauer, R.; Spur, G.: „Handbuch Umformen“, Carl Hanser, München, 2012
[2] Osakada, K.; Mori, K.; Altan, T.; Groche, P.: “Mechanical servo press technology for metal forming”, CIRP Annals - Manufacturing Technology, vol. 60, 2011, pp. 651-672
[3] Altan, T.; Groseclose, A.; Billur, E.; Subramonian, S.; Mao, T.: “Advances and challenges in sheet metal forming technology”, 7th International Conference on Design and Production of Machines and Dies/Molds, Antalya, Turkey, 2013, pp 1-6
[4] Del Pozo, D.; López de Lacalle, L.N.; López, J.M.; Hernández, A.: “Prediction of press/die deformation for an accurate manufacturing of drawing dies”, The International Journal of Advanced Manufacturing Technology, vol. 37, 2008, pp. 649-656
[5] Swidergal, K.; Lubeseder, C.; von Wurmb, I.; Lipp, A.; Meinhardt, J.; Wagner, M.; Marburg, S.: "Experimental and numerical investigation of blankholder's vibration in a forming tool: A coupled MBS-FEM approach", Production Engineering, (in review process)
[6] Hardtmann, A.: “Entwicklung und Bewertung eines erweiterten Blechumformprozessmodells unter besonderer Berücksichtigung der elasto-statischen Wechselwirkungen zwischen Maschine und Prozess“, PhD thesis, Technische Universität Dresden, 2010
[7] ANSA User's Guide, BETA CAE Systems SA, 2015
[8] LS-DYNA User Manual and Theoretical Manual, Livermore Software Technology Corporation
[9] Benson, D.J.; Kolling, S.; Du Bois, P.A.: “A simplified approach for strain-rate dependent hyperelastic materials with damage”, 9th International LS-DYNA Users Conference, Dearborn, MI, USA, 4.-6. June 2006
[10] Swidergal, K.; Thumann, P.; Lubeseder, C.; von Wurmb, I.; Meinhardt, J.; Wagner, M.; Marburg, S.: “Modeling and simulation of carbon black filled elastomer damper using LS-DYNA”, 13. LS-DYNA Forum, Bamberg, Germany, 6.-8. October 2014
[11] Mullins L.J.: “Effect of stretching on the properties of rubber”, Journal of Rubber Research, vol. 16, 1947, pp. 275-289
[12] Haufe, A.; Lorenz, D.; Roll, K.; Bogon, P.: „Concepts to take elastic tool deformations in sheet metal forming into account”, 10. International LS-DYNA Users Conference, Dearborn, MI, USA, 8.-10. June 2008